Supporting Information

Self-Assembly of Block Copolymers during Hollow Fiber Spinning: An *In Situ* Small-Angle X-Ray Scattering Study

Kirti Sankhala[1], D. C. Florian Wieland[2], Joachim Koll[1], Maryam Radjabian[1], Clarissa Abetz[1], Volker Abetz[1,3*]

[1] Helmholtz-Zentrum Geesthacht, Institute of Polymer Research, Max-Planck-Strasse 1, 21502 Geesthacht, Germany

[2] Helmholtz-Zentrum Geesthacht, Institute of Materials Research, Max-Planck-Strasse 1, 21502 Geesthacht, Germany

[3] University of Hamburg, Institute of Physical Chemistry, Martin-Luther-King-Platz 6, 20146 Hamburg, Germany

[*]E-mail: volker.abetz@hzg.de

1. Preparation of polymer solutions

The PS-*b*-P4VP diblock copolymers were synthesized via sequential anionic polymerization following a protocol reported before.[1] The number average molar mass (M_n) and dispersity index ($Đ$) of the polystyrene precursor and the diblock copolymers were measured by gel permeation chromatography (GPC) (Waters 2410 refractive-index detector, *N,N*-dimethylacetamide as eluent) at 50 °C which was calibrated against polystyrene standards. The composition of the block copolymer was determined by ^{1}H nuclear magnetic resonance spectroscopy (^{1}H NMR) (in deuterated chloroform) on a Bruker advance 300 NMR spectrometer. Using the composition and the molecular weight of the PS precursor the total molecular weight of the block copolymer was calculated. All chemicals used in this study were purchased either from Sigma-Aldrich or from Merck. The solutions were prepared by stirring a specific concentration of block copolymer in a mixture of DMF/THF in equal weight ratio (wt/wt); all measurements were done in wt%. To assure the homogeneity in solutions, we stirred the solutions at least for 72 hours and allowed to rest for some hours.

2. Preparation of bulk films and their characterization

For the investigation of the bulk morphology of the PS-*b*-P4VP diblock copolymers films were prepared from solution. The solutions were prepared by stirring 160 mg of block copolymer in 2.5 mL of chloroform for 24 hours. The homogeneous solutions were transferred into polytetrafluoroethylene (PTFE) molds and kept for drying in a hood for two days. In order to equilibrate the sample, *i.e.*, to remove the solvent effect and air bubbles trapped in the samples; the films were further annealed at temperatures below and above the glass transition temperature of both blocks under vacuum. The temperature was gradually increased to 140 °C near the glass transition of P4VP block and finally the samples were annealed for 4 h at 170 °C. The sections from the same films were used for characterization by SAXS and TEM.

Transmission Electron Microscopy

The morphology of the diblock copolymer microdomains was observed by TEM using a Tecnai G2 F20 (FEI, Eindhoven, The Netherlands) operated at 120 kV in bright-field mode. For this, the films were embedded in epoxy and ultrathin sections of ca. 50 nm thickness were obtained by using a Leica Ultramicrotome EM UCT (Leica Microsystems, Wetzlar, Germany) equipped with a diamond knife (Diatome AG, Biel, Switzerland) was utilized. The ultrathin sections were stained with I_2 vapor for 1 hour.

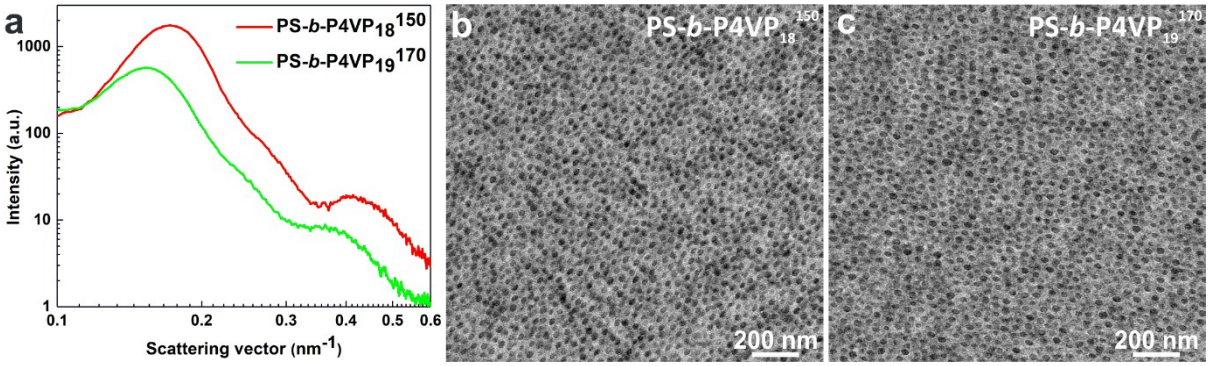

Fig. S1. Bulk characterization. (a) SAXS curves of the diblock copolymers. The SAXS curves are plotted in log-log scale and Intensity-offset is adjusted for better visibility. (b,c) TEM micrographs of the bulk films as described in the text.

From the SAXS curves shown in Fig. S1a, the domain spacing (d_{bulk}) determined from the primary peak corresponding to the scattering vector q^* is 36.5 ± 0.6 nm in PS-*b*-P4VP$_{18}^{150}$ and 41.2 ± 0.6 nm in PS-*b*-P4VP$_{19}^{170}$ (Table 1).

TEM was employed to obtain a direct visualization of the bulk morphology and there by provide insight regarding the spheres. The values of average center-to-center distance between spherical domains were checked manually using DigitalMicrograph (Gatan Microscopy Suite Software, Gatan GmbH, München, Germany), which is 39 ± 6 nm in PS-*b*-P4VP$_{18}^{150}$ and 44 ± 8 nm in PS-*b*-P4VP$_{19}^{170}$, measured from Fig. S1 b and c, respectively. These values are in agreement with the d_{bulk} measured from SAXS. It is worth noting here that the preparation artifacts during sample preparation for TEM might lead to stretching or compression in different directions. In case of SAXS characterization, the average of scattering from the full film is in one direction. In addition, the X-ray beam has a diameter of 350 µm that makes the probed sample quite large for SAXS as compared to the sample investigated by TEM.

3. SAXS of Solutions

Table S1. Details of SAXS curves of PS-*b*-P4VP$_{19}^{170}$ block copolymer solutions, as shown in Fig. 2a. All q^* and d have an error bar of ± 0.001 nm^{-1} and ± 0.4 nm, respectively.

Polymer solution	Scattering vector q (nm^{-1})			$(q/q^*)^2$			d (nm)
	1st (q^*)	2nd	3rd	1st	2nd	3rd	1st
21 wt% PS-*b*-P4VP$_{19}^{170}$ and 1.5 wt% $MgAc_2$	0.114	0.161	0.198	1	1.9967	3.0042	55.1
23 wt% PS-*b*-P4VP$_{19}^{170}$ and 1.0 wt% $MgAc_2$	0.114	0.162	0.198	1	2.0054	2.9997	55.1
28 wt% PS-*b*-P4VP$_{19}^{170}$	0.117	0.166	0.202	1	2.0063	2.9946	53.7
25 wt% PS-*b*-P4VP$_{19}^{170}$	0.120			1			52.3

4. Analysis of SEM micrographs

To obtain the average pore diameter (D_p) and the average center-to-center distance between pores (d_{c-c}), the SEM micrographs were analyzed by the image analysis software analySIS (Olympus Soft Imaging Solutions GmbH, Münster, Germany), presented in Table S2 as 'Analysis 1'. In this, the values D_p and d_{c-c} were generated by differentiating the grey level intensity (threshold) of the SEM image. The SEM micrographs representing the membranes cast for an evaporation time of 2 seconds have a high number of closed or partially open pores, which decreases the D_p value. So, in order to determine the similarity of the pore distribution and the size of pore forming microdomains (from the contrast of grey level of pore-forming domains), the SEM micrographs were also processed by DigitalMicrograph, by performing an autocorrelation. This provides a visual impression of average periodic arrangements of pores with information about D_p and d_{c-c}, as shown in column 'Analysis 2', in Table S2. Here, D_p is calculated by calculating the diameter of the central bright spot and d_{c-c} is calculated by taking the average of distances between the central bright spot to all nearest bright spots (located in first ring).The autocorrelation data is more appropriate for the highly periodic pore patterns. The pixel size of SEM micrograph is mentioned as the error in measurement, *i.e.*, ca. 3 nm. In both the methods, the calculated d_{c-c} values are almost equal.

Table S2. Analysis of SEM micrographs. *Analysis 1* is done by analySIS and *Analysis 2* is done using DigitalMicrograph by performing autocorrelation. D_p is average pore diameter and d_{c-c} is average center-to-center distance between pores.

Polymer solution in DMF/THF 50/50 (wt/wt)	Evaporation time (SEM micrograph)	*Analysis 1* (AnalySIS)		*Analysis 2* (DigitalMicrograph)	
		D_p (nm)	d_{c-c} (nm)	D_p (nm)	d_{c-c} (nm)
26 wt% PS-*b*-P4VP$_{18}^{150}$	2 s (Fig. 1b)	12 ± 3	47 ± 4	25 ± 3	48 ± 3
26 wt% PS-*b*-P4VP$_{18}^{150}$	5 s (Fig. 1c)	19 ± 3	47 ± 2	20 ± 3	49 ± 3
25 wt% PS-*b*-P4VP$_{19}^{170}$	2 s (Fig. 1e/2b)	16 ± 5	58 ± 5	30 ± 3	59 ± 3
25 wt% PS-*b*-P4VP$_{19}^{170}$	5 s (Fig. 1f)	25 ± 3	55 ± 2	24 ± 3	53 ± 3
28 wt% PS-*b*-P4VP$_{19}^{170}$	2 s (Fig. 2c)	18 ± 5	54 ± 5	30 ± 3	55 ± 3
23 wt% PS-*b*-P4VP$_{19}^{170}$ and 1.0 wt% $MgAc_2$	2 s (Fig. 2d)	18 ± 6	56 ± 8	33 ± 3	58 ± 3
21 wt% PS-*b*-P4VP$_{19}^{170}$ and 1.5 wt% $MgAc_2$	2 s (Fig. 2e)	18 ± 6	55 ± 4	32 ± 3	56 ± 3

5. SAXS curves of as-spun HFM

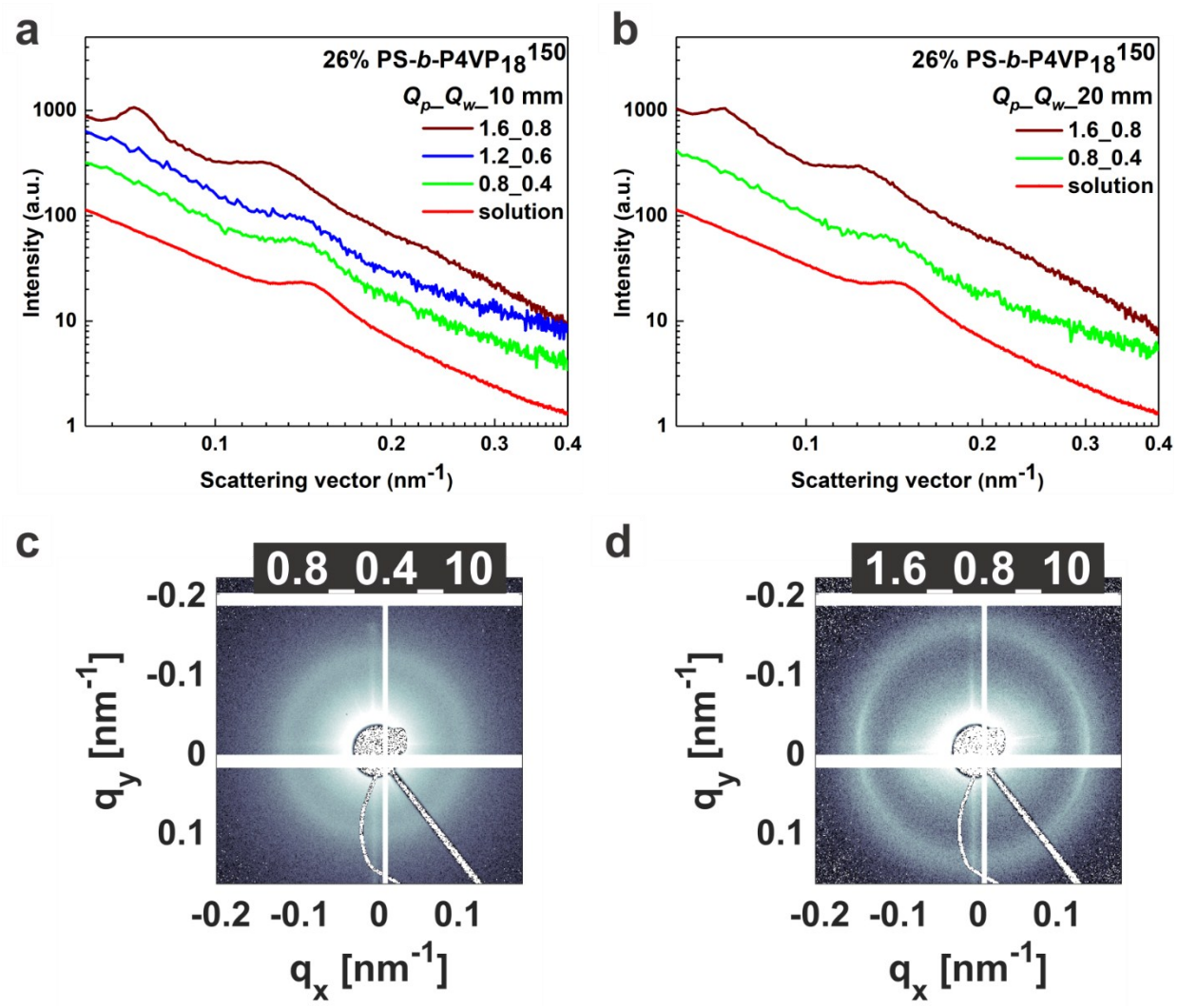

Fig. S2. **Influence of Q_p.** (a,b) SAXS curves and (c,d) SAXS patterns of as-spun HF using block copolymer solution 26 wt% PS-*b*-P4VP$_{18}$^{150} in DMF/THF 50/50 (wt/wt) at a particular set of spinning parameters, polymer flow rate Q_p (mL/min), bore fluid flow rate Q_w (mL/min) and air gap distance L_a (mm), mentioned as $Q_p\_Q_w\_L_a$. The SAXS data are plotted in log-log scale and Y-offset is adjusted for clarity. (c,d) The images show the ring originating from the domain correlation. The fiber runs in the vertical direction and is slightly tilted due to the movement of the precipitation bath.

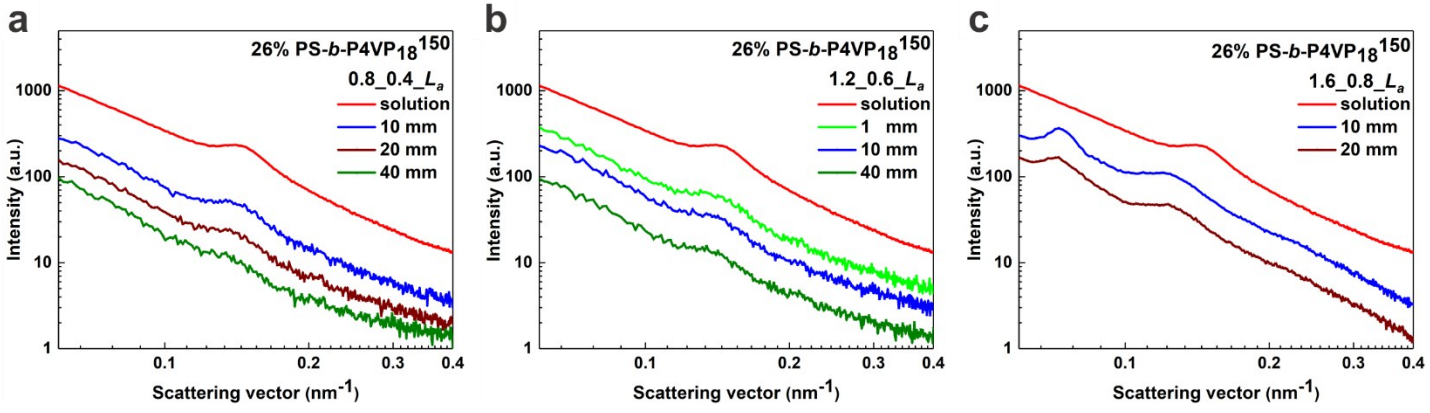

Fig. S3. Influence of L_a. SAXS curves of as-spun HF using block copolymer solution 26 wt% PS-*b*-P4VP$_{18}^{150}$ in DMF/THF 50/50 (wt/wt) at different L_a (mm) for a particular set of Q_p_Q_w (in mL/min): 0.8_0.4 (a); 1.2_0.6 (b) 1.6_0.8 (c). The SAXS data are plotted in log-log scale and Intensity-offset is adjusted for clarity.

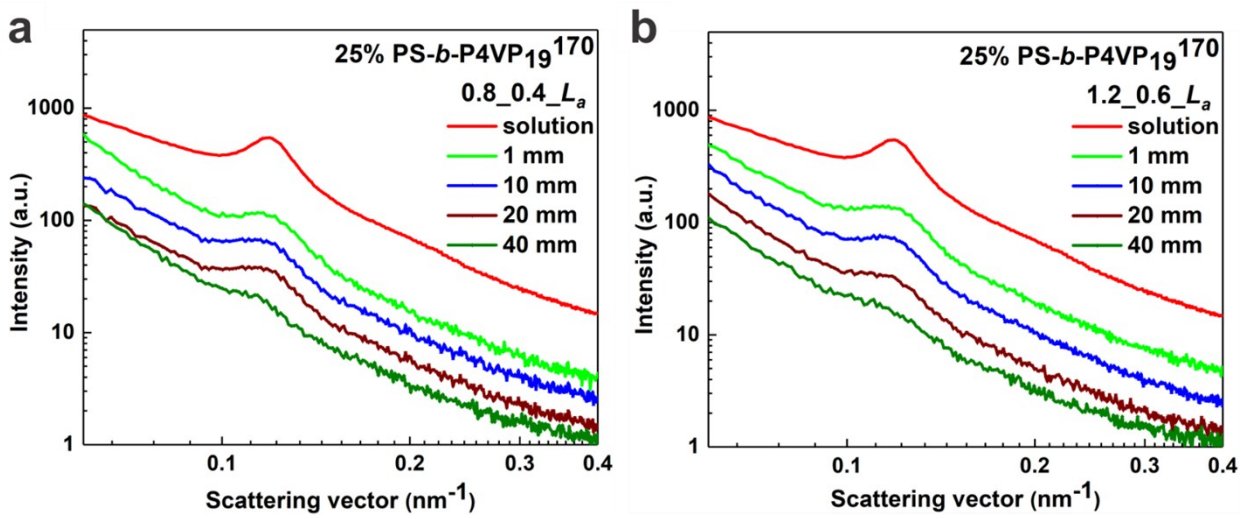

Fig. S4. **Influence of L_a.** (a,b) SAXS curves of as-spun HF using block copolymer solution 25 wt% PS-*b*-P4VP$_{19}^{170}$ in DMF/THF 50/50 (wt/wt) at different L_a (mm) for a particular set of Q_p_Q_w (mL/min): 0.8_0.4 (a); 1.2_0.6 (b). The SAXS data are plotted in log-log scale and Intensity-offset is adjusted for clarity.

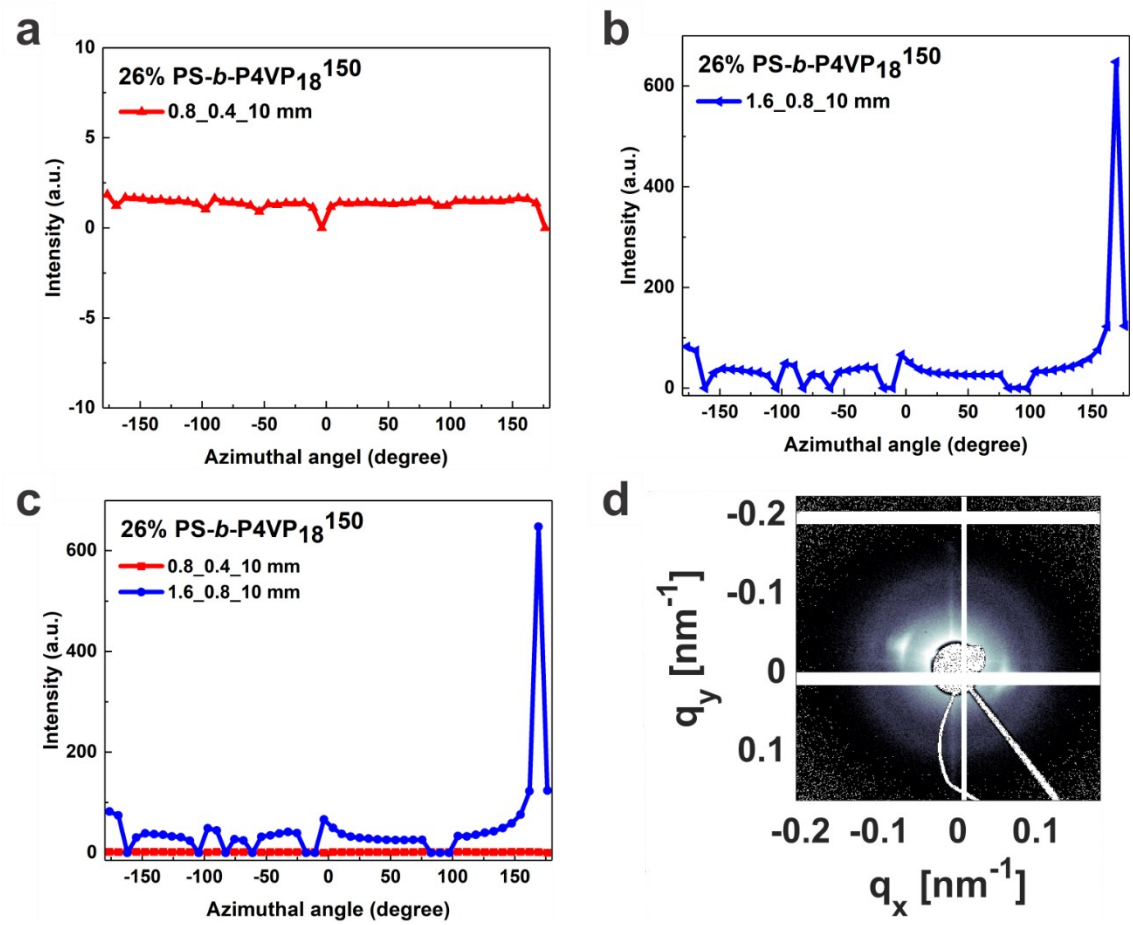

Fig. S5. **Influence of Q_p.** 1D azimuthal intensity curves of as-spun HF using block copolymer solution 26 wt% PS-*b*-P4VP$_{18}^{150}$ in DMF/THF 50/50 (wt/wt) at a particular L_a of 10 mm for different Q_p_Q_w: 0.8_0.4 (a) and 1.6_0.8 (mL/min) (b). (c) Stacked curves. We note that in the azimuthally integrated data only one peak can be observed. This is due to the fact that the other peak lies on a dead area of the pilatus detector making it impossible to see.

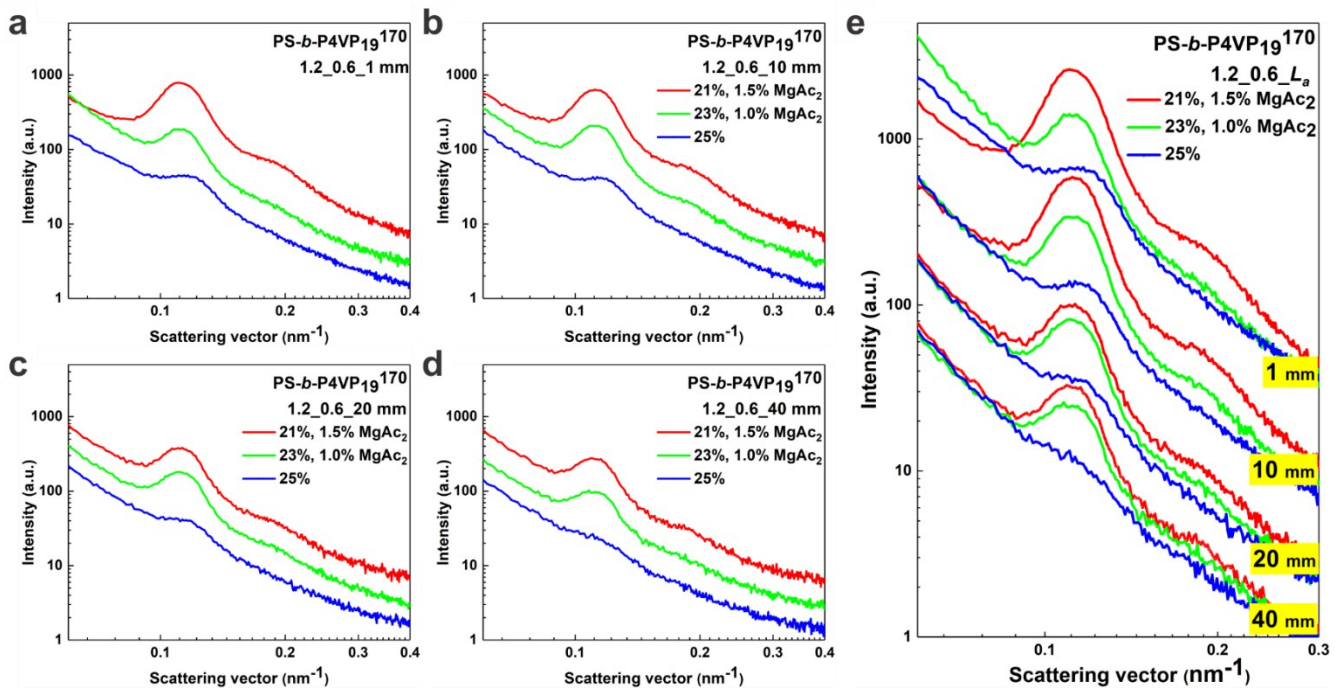

Fig. S6. **Influence of polymer solution.** (a-d) SAXS curves of as-spun HF using different block copolymer solutions 25 wt% PS-*b*-P4VP$_{19}^{170}$, 23 wt% PS-*b*-P4VP$_{19}^{170}$ and 1.0 wt% $MgAc_2$ and 21 wt% PS-*b*-P4VP$_{19}^{170}$ and 1.5 wt% $MgAc_2$ in DMF/THF 50/50 (wt/wt). The curves are plotted for Q_p 1.2 mL/min and Q_w 0.6 mL/min, at different L_a: 1 mm (a); 10 mm (b); 20 mm (c); 40 mm (d). (e) The sets of SAXS curves a-d are stacked together. The SAXS data are plotted in log-log scale and Intensity-offset is adjusted for clarity.

6. SEM micrographs of HFM and the analysis

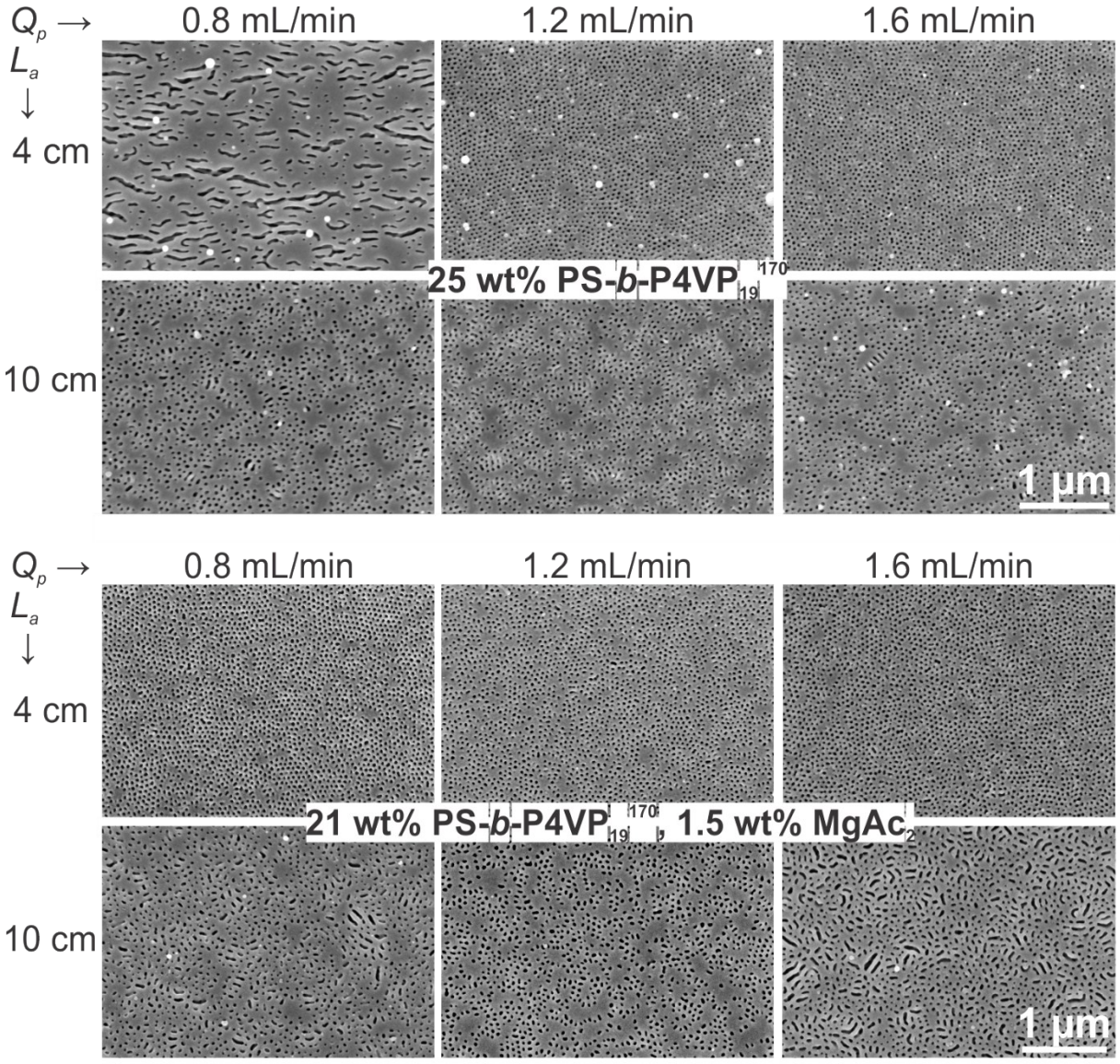

Fig. S7. The SEM micrographs show the influence of spinning parameters (Q_p_Q_w_L_a) on the morphology of the outer surface of HFM. The HFM were spun using block copolymer solutions of 25 wt% PS-*b*-P4VP$_{19}$^{170} and 21 wt% PS-*b*-P4VP$_{19}$^{170} and 1.5 wt% $MgAc_2$ in DMF/THF 50/50 (wt/wt) for Q_p 0.8, 1.2 and 1.6 mL/min, at L_a 40 and 100 mm.

Table S3. Analysis of SEM micrographs of outer surface of HFM, as shown in Fig. S7, is done by analySIS. D_p is average pore diameter and $d_{c\text{-}c}$ is average center-to-center distance between pores.

25 wt% PS-*b*-P4VP$_{19}^{170}$						
Q_p ⊠ L_a ⊠	0.8 mL/min		1.2 mL/min		1.6 mL/min	
	D_p (nm)	$d_{c\text{-}c}$ (nm)	D_p (nm)	$d_{c\text{-}c}$ (nm)	D_p (nm)	$d_{c\text{-}c}$ (nm)
40 mm			23 ± 5	56 ± 4	23 ± 5	56 ± 4
100 mm	26 ± 10	63 ± 4	29 ± 6	61 ± 4	31 ± 9	61 ± 4
21 wt% PS-*b*-P4VP$_{19}^{170}$ and 1.5 wt% $MgAc_2$						
Q_p ⊠ L_a ⊠	0.8 mL/min		1.2 mL/min		1.6 mL/min	
	D_p (nm)	$d_{c\text{-}c}$ (nm)	D_p(nm)	$d_{c\text{-}c}$ (nm)	D_p (nm)	$d_{c\text{-}c}$ (nm)
40 mm	28 ± 5	55 ± 4	26 ± 6	57 ± 5	24 ± 6 nm	55 ± 4
100 mm	29 ± 14	61 ± 5	35 ± 10	62 ± 4	28 ± 8 nm	62 ± 4

Table S4. Analysis of SEM micrographs of cross-sections of HFM, as shown in Figs. 5 and 7. D_{out} is outer diameter and D_{in} is inner diameter of HFM.

25 wt% PS-*b*-P4VP$_{19}^{170}$						
Q_p ⊠ L_a ⊠	0.8 mL/min	1.2 mL/min	1.6 mL/min	0.8 mL/min	1.2 mL/min	1.6 mL/min
	D_{out} (µm)			D_{in} (µm)		
40 mm	1006 ± 20	1069 ± 66	1037 ± 12	678 ± 32	735 ± 74	773 ± 10
100 mm	686 ± 3	785 ± 51	809 ± 33	439 ± 47	545 ± 54	584 ± 33
21 wt% PS-*b*-P4VP$_{19}^{170}$ and 1.5 wt% $MgAc_2$						
Q_p ⊠ L_a ⊠	0.8 mL/min	1.2 mL/min	1.6 mL/min	0.8 mL/min	1.2 mL/min	1.6 mL/min
	D_{out} (µm)			D_{in} (µm)		
40 mm	961 ± 66	873 ± 68	935 ± 76	733 ± 73	645 ± 32	700 ± 76
100 mm	687 ± 43	712 ± 19	673 ± 54	515 ± 42	468 ± 19	435 ± 40

Reference

1. S. Rangou, K. Buhr, V. Filiz, J. I. Clodt, B. Lademann, J. Hahn, A. Jung and V. Abetz, *J. Membr. Sci.*, 2014, **451**, 266-275.